中国科学院新疆天文台
XINJIANG ASTRONOMICAL OBSERVATORY, CAS

Acceleration and Collimation Zone (ACZ) of the NGC 4261 Jet: A Scaled-down Counterpart to M87?

Xi YAN

Xinjiang Astronomical Observatory (XAO)

Collaborators: Lang CUI, Kazuhiro Hada, Sandor Frey, Rusen Lu, Wu Jiang, Zhiqiang Shen, Luis C. Ho, et al.

2025.10, Bologna, Italy

Outline

- ❑ Background
- ❑ Subparsec Acceleration and Collimation of NGC 4261's Twin Jets
- ❑ Summary and Outlook

1. Background

- **Low-luminosity AGNs (LLAGNs; e.g., Ho, 2008):**
  - Very common in the local universe (> 30%)
  - Low bolometric luminosity ($L_{\rm bol} \leq 10^{42}$ erg/s)
  - Low radiation efficiency (<< 0.1)
  - Low accretion rate ($L_{\rm bol}/L_{\rm Edd} \approx 10^{-6} \sim 10^{-3}$)
  - Radio loud
  - Abnormal SED and spectral lines

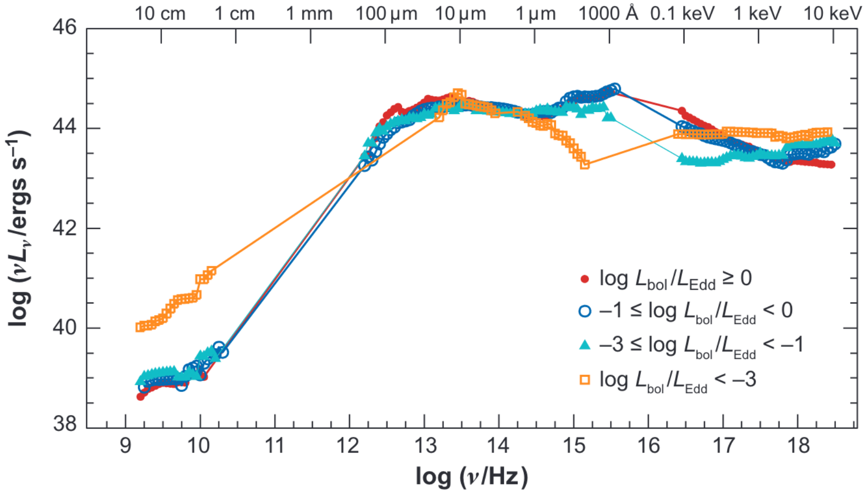

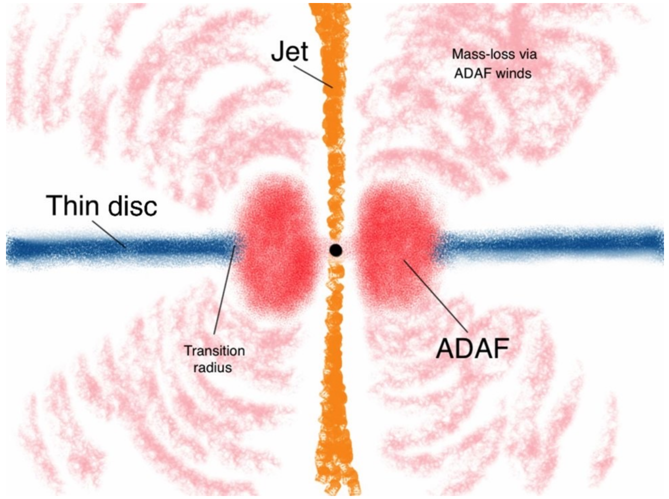

Ho, (2008); Nemmen et al., (2014)

1. Background

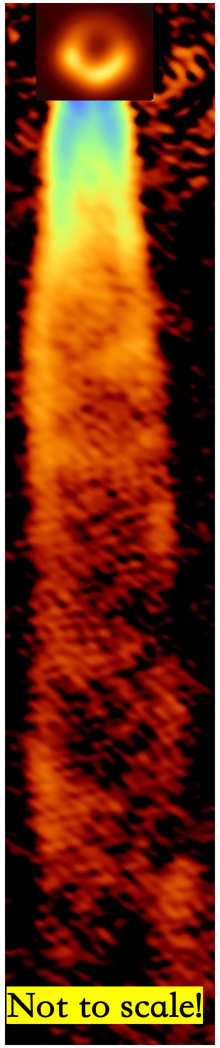

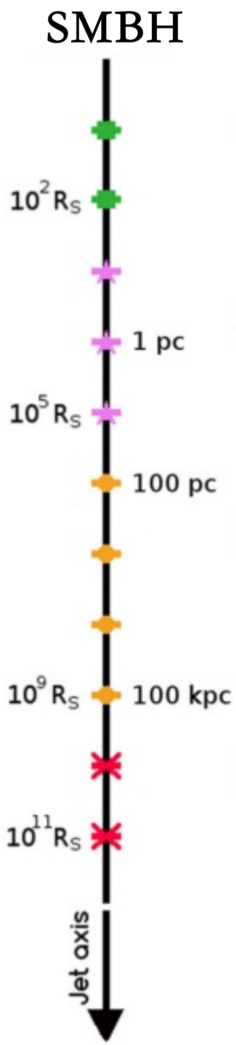

Formation region → (sub)mm-VLBI： SMBH、ADAF、Jet base

Acceleration and Collimation Zone (ACZ) → Multi-frequencies: jet collimation

Multi-epochs: jet acceleration

Kinematic energy dominated

Dissipation

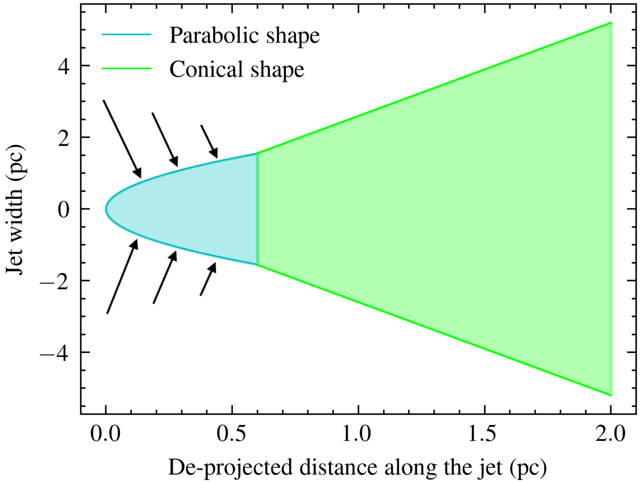

$W \propto r^a$

$a = 0$ → Cylindrical
$a = 0.5$ → Parabolic
$a = 1$ → Conical

Boccardi et al. (2017)； Walker et al. (2018)； EHTC (2019)

1. Background

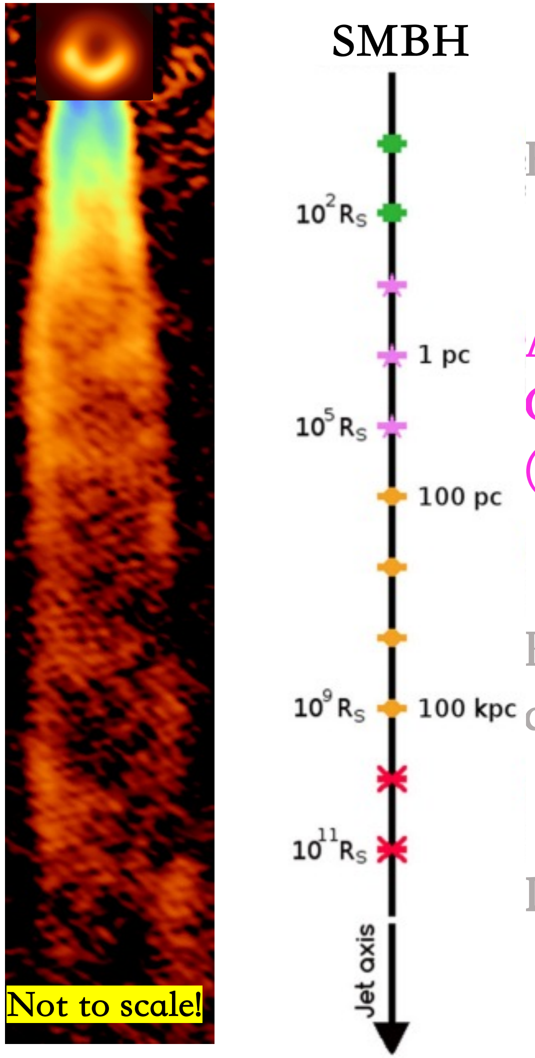

Formation region

Acceleration and Collimation Zone (ACZ)

Kinematic energy dominated

Dissipation

Boccardi et al. (2017); Walker et al. (2018); EHTC (2019)

M87

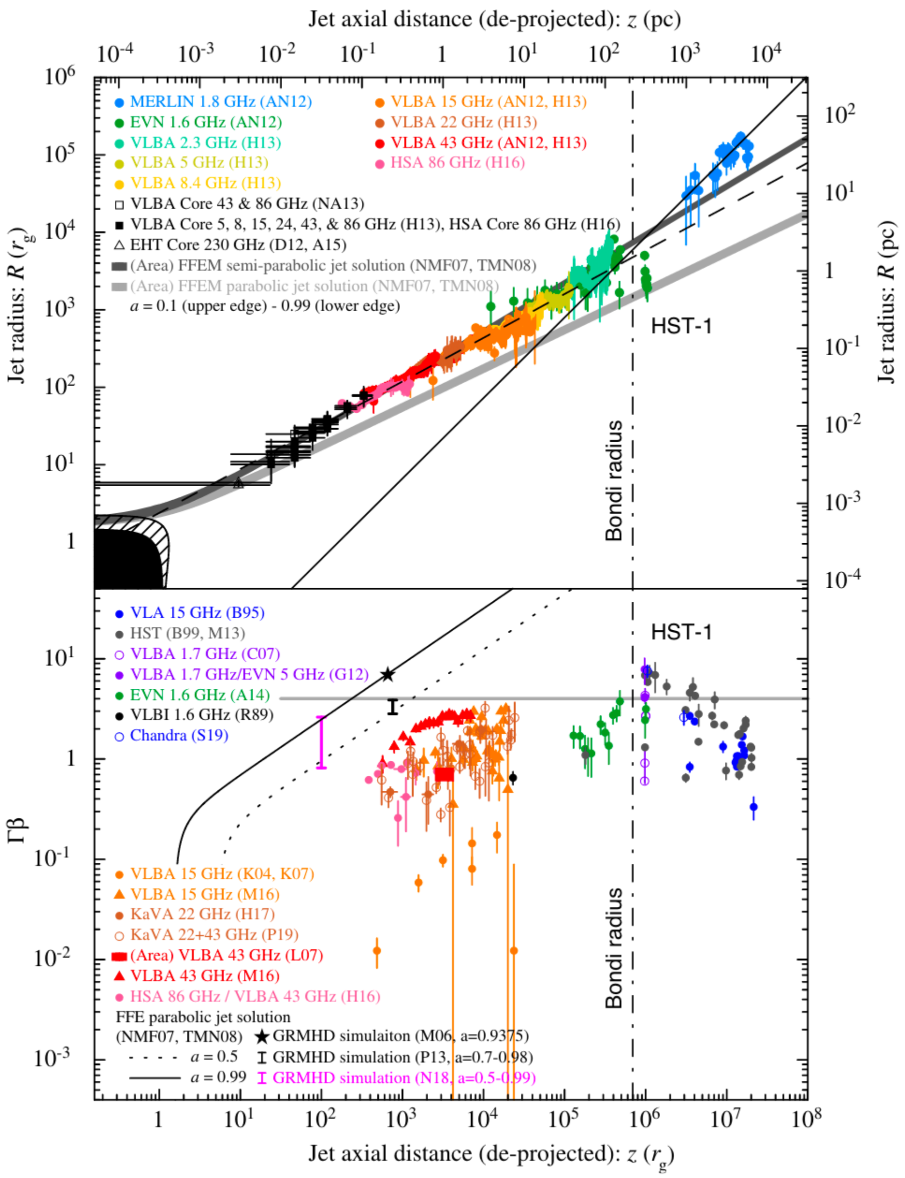

Asada and Nakamura (2012)
Park et al. (2019)
Hada et al. (2024)

1. Background

➢Only four AGNs show firm evidence of concurrent ACZ:

- M 87 (LLAGN; Park et al. 2019)
- NGC 315 (LLAGN; Park et al. 2021, 2024; Boccardi et al. 2021; Ricci et al. 2022)
- 1H 0323+342 (NLS1 galaxy; Hada et al. 2018)
- 1928+738 (FSRQ; Yi et al. 2024)

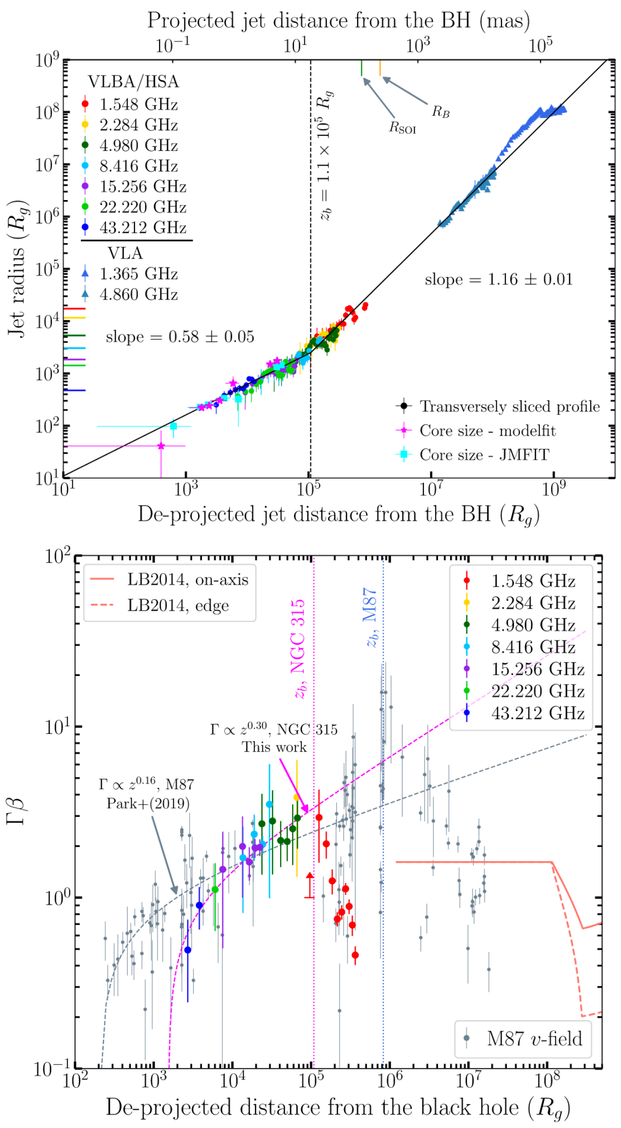

NGC 315

1. Background

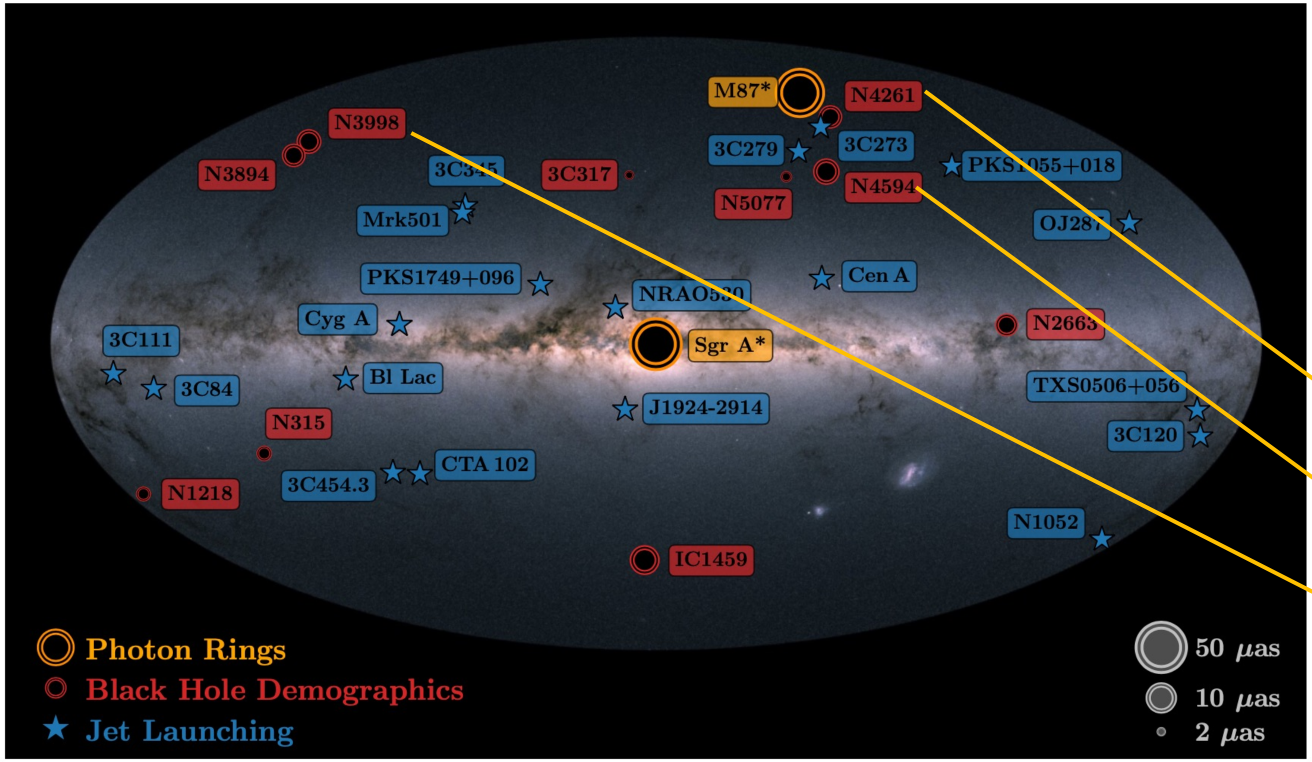

Figure 3. **Potential BHEX targets.** Horizon-scale targets are shown as rings, scaled (logarithmically) by the expected angular size of the black hole shadow. The primary targets for photon ring studies and direct measurements of spin, Sgr A* and M87*, are shown in orange. The remaining horizon-scale targets, shown in red, include a variety of sources in low accretion states, sampling both radio-loud and radio-quiet sources.[94] In addition, BHEX will study a wide variety of AGN with prominent jets, including potential binary supermassive black holes (e.g., OJ287), sources associated with neutrino emission (TXS0506+056), and bright gamma-ray blazars with superluminal features (e.g., 3C279, CTA102). Many of these sources have already been studied with the EHT.[95–99] Background image: ESA/Gaia/DPAC.

Johnson et al. (2024)

- How about the ACZ properties in other AGNs?
- ngEHT SMBH imaging candidates
  - NGC 4261
  - NGC 4594 (M 104, Sombrero galaxy)
  - NGC 3998

Yan et al. (2023, 2024, 2025a, 2025b)

1. Background

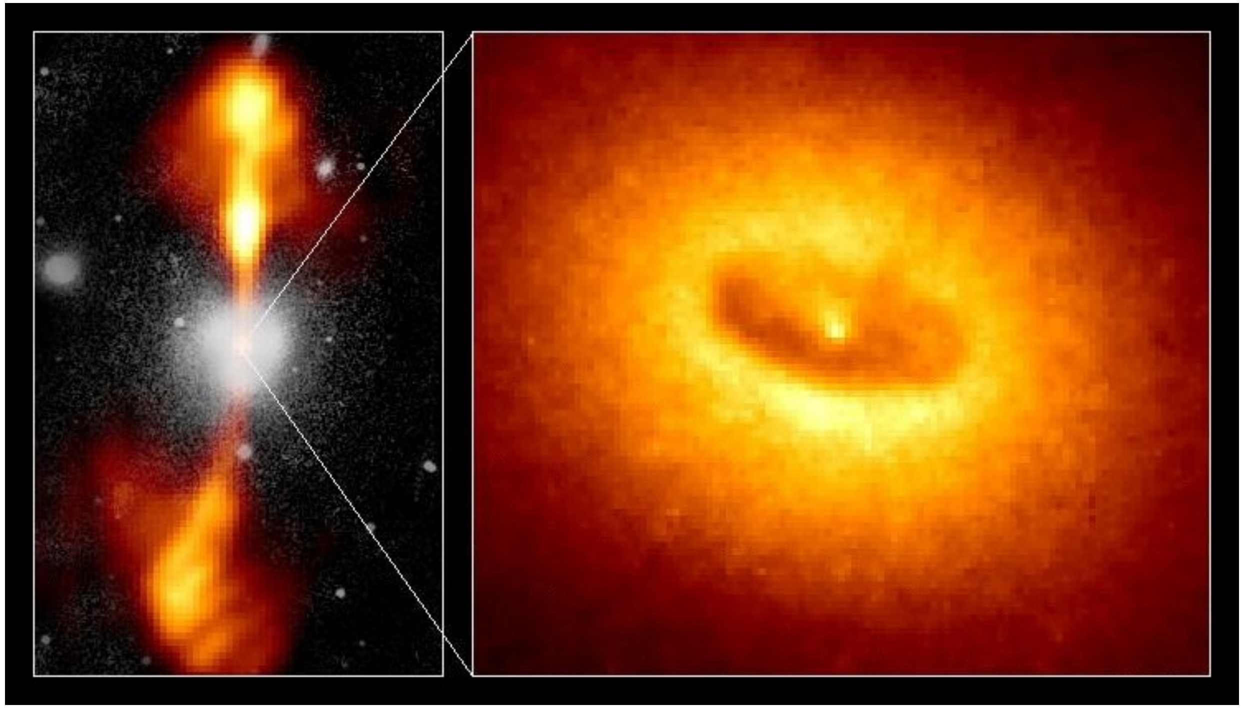

A VLA + HST view of NGC 4261

	NGC 4261
L_{bol} (erg s^{-1})	1.4×10^{42}
L_{bol}/L_{Edd}	2.5×10^{-5}
D (Mpc)	31.6
M_{BH} ($M_\odot$)	1.62×10^{9}
Scale	1 mas ~ 0.15 pc ~ 988 R_s

Jaffe et al. (1993); Ho et al., (1997b, 1999b) ; Tonry et al. (2001); Sutter and Fadda, (2022)

2.1 Archival VLBA Datasets

- ➢Freq. 1.4 - 88 GHz
- ➢Time: 1995 - 2022

Table 1
Summary of NGC 4261 Observations

Freq. (GHz)	P.C.	Date	Array	Pol	Bandwidth (MHz)	Beam Size (mas × mas, deg)
15	BM166	2002.07.05	VLBA	Dual	64	0.922 × 0.512, −4.3
15	BM175b	2002.09.27	VLBA	LCP	64	1.04 × 0.498, −5.1
15	BM175c	2003.05.05	VLBA	LCP	64	1.01 × 0.456, −5.12
15	BM175a	2003.07.04	VLBA	LCP	64	1.02 × 0.459, −4.66
43	BM215a	2004.12.20	VLBA	Dual	64	0.344 × 0.175, −8.31
44	BY167	2022.02.14	VLBA, -SC,-HN	Dual	1024	0.627 × 0.171, −22.4
88	BY167	2022.02.14	VLBA, -SC,-HN	Dual	1024	0.467 × 0.101, −19.2

Note. Column (1): Observing frequency. Column (2): Project code. Column (3): Date of observation. Column (4): Participatin
indicated with a minus sign. Column (5): Polarization. Column (6): Bandwidth. Column (7): FWHM and position angle of the
Peak intensity and rms noise.

Yan et al. (2023, 2025)

Table 1. Summary of the Observations and Data of NGC 4261

P.C. (1)	Freq. (GHz) (2)	Epoch (3)	Array (4)	Pol. (5)	B.W. (MHz) (6)	$T_{\rm int}$ (min) (7)	$\theta_{\rm maj} \times \theta_{\rm min}$, PA (mas × mas, ∘) (8)	$I_{\rm peak}$ (mJy/B) (9)	$I_{\rm rms}$ (mJy/B) (10)	$S_{\rm tot}$ (mJy) (11)	Publication (12)
BW011	1.7	1995/04/01	VLBA (MK†, SC†)	LCP	64	∼ 235	9.75 × 5.14, 10.6	78.6	0.25	190.9 ± 19.1	(1),(2) (3),(4)
	8.4		VLBA	RCP	64	∼ 75	1.92 × 0.86, 1.7	121.1	0.30	349.5 ± 35.0	
BJ028	8.4	1999/02/26	VLBA	RCP	64	∼ 475	1.69 × 0.73, −3.7	99.8	0.10	298.5 ± 29.9	(4)
	8.4	1999/10/21	VLBA, −BR	RCP	64	∼ 460	2.06 × 0.70, −8.8	124.3	0.11	331.8 ± 33.2	
BS094b	1.4	2002/08/29	VLBA, −BR	Dual	32	∼ 60	10.99 × 4.54, −3.7	55.6	0.30	149.8 ± 15.0	...
	2.3			RCP	16	∼ 60	7.01 × 2.85, −4.8	97.1	0.45	209.9 ± 21.0	
	5.0			LCP	32	∼ 60	3.13 × 1.26, −4.7	113.5	0.30	300.4 ± 30.0	
	8.4			RCP	16	∼ 60	1.98 × 0.79, −4.3	145.8	0.55	316.6 ± 31.7	
BA064	4.8	2002/12/14	VLBA (FD, KP, LA, NL, OV, PT)	Dual	64	∼ 25	9.02 × 4.27, −20.7	202.0	0.49	304.1 ± 30.4	...
	8.3			Dual	64	∼ 25	5.40 × 2.59, −20.6	221.8	0.46	337.2 ± 33.7	
BS094c	15	2003/06/28	VLBA	LCP	32	∼ 60	0.97 × 0.43, −0.2	125.1	0.81	306.5 ± 30.7	(5) (6) (7)
	22					∼ 60	0.66 × 0.26, −1.7	122.4	1.30	283.0 ± 28.3	
	43					∼ 60	0.35 × 0.16, 2.7	135.7	2.30	271.4 ± 27.1	
BS094d	1.4	2003/07/05	VLBA	Dual	32	∼ 60	9.70 × 4.63, −1.2	54.1	0.50	162.3 ± 16.2	(5) (6) (7)
	2.3			RCP	16	∼ 60	6.15 × 2.95, −2.4	98.6	0.50	221.9 ± 22.2	
	5.0			LCP	32	∼ 60	2.82 × 1.33, −4.1	122.2	0.26	295.5 ± 29.6	
	8.4			RCP	16	∼ 60	1.77 × 0.80, −3.0	121.5	0.50	299.0 ± 29.9	

NOTE— Column (1): project code. Note that the BS094b/c/d are phase-referencing observations (see details in T. Haga et al. 2015). Column (2): frequency. Column (3): observation date. Column (4): participating stations (stations not participated are marked with a minus sign). †: the fringe detection is marginal. Column (5): polarization. LCP – Left Circular Polarization; RCP – Right Circular Polarization; Dual – LCP and RCP. Column (6): bandwidth. Column (7): on-source integration time. Column (8): Full Width at Half Maximum (FWHM) of the synthesized beam's major and minor axes, along with the position angle (PA) of the major axis. Columns (9)-(11): peak intensity, rms noise level (σ), and total flux density of the CLEAN image. Column (12): publications in which the data have been used: (1) D. L. Jones & A. E. Wehrle (1997); (2) D. L. Jones et al. (2000); (3) D. L. Jones et al. (2001); (4) B. G. Piner et al. (2001); (5) T. Haga et al. (2015); (6) N18; (7) Y23. Note that the BS094c/d datasets have been used to measure the core shift and jet collimation profile (see T. Haga et al. 2015; N18; Y23).

2.2 Jet Morphology

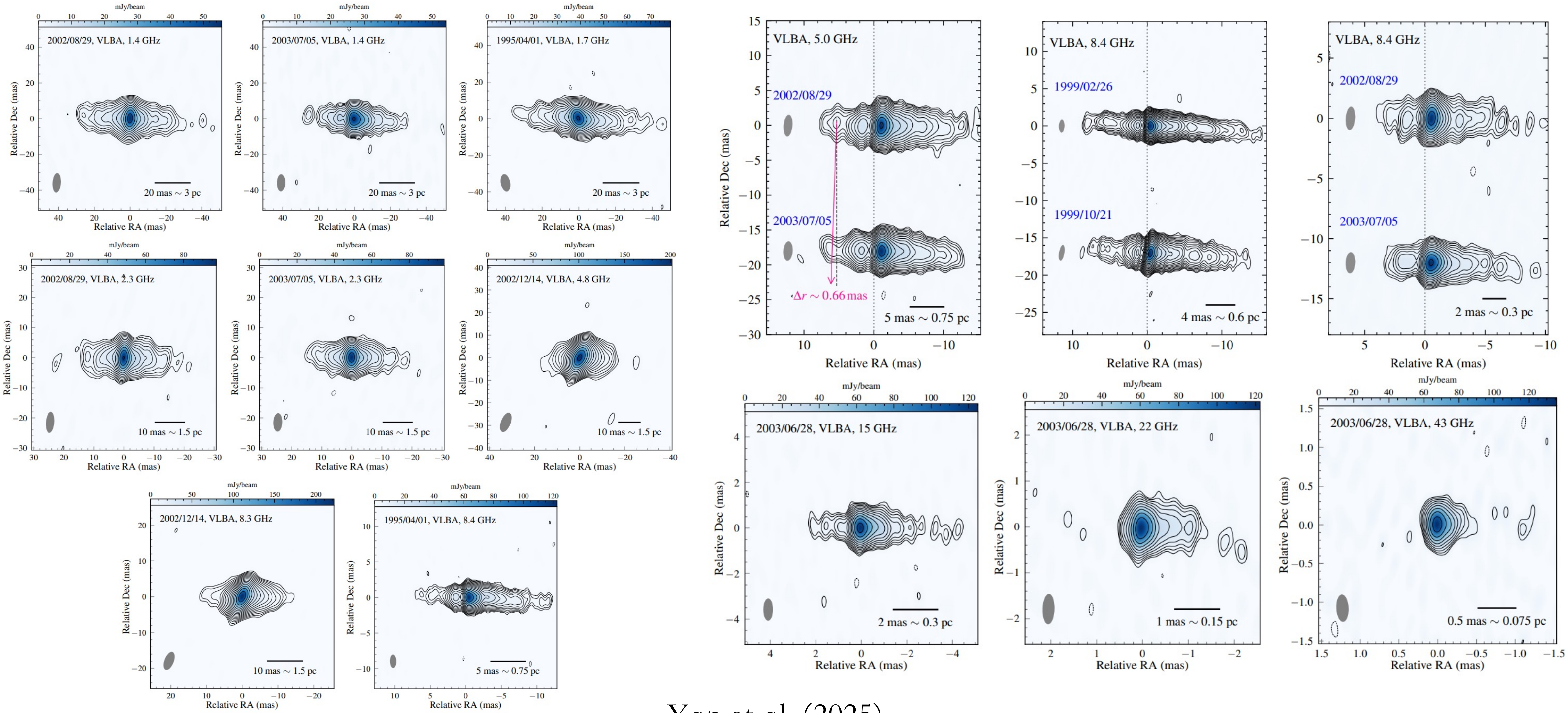

Yan et al. (2025)

2.2 Jet Morphology

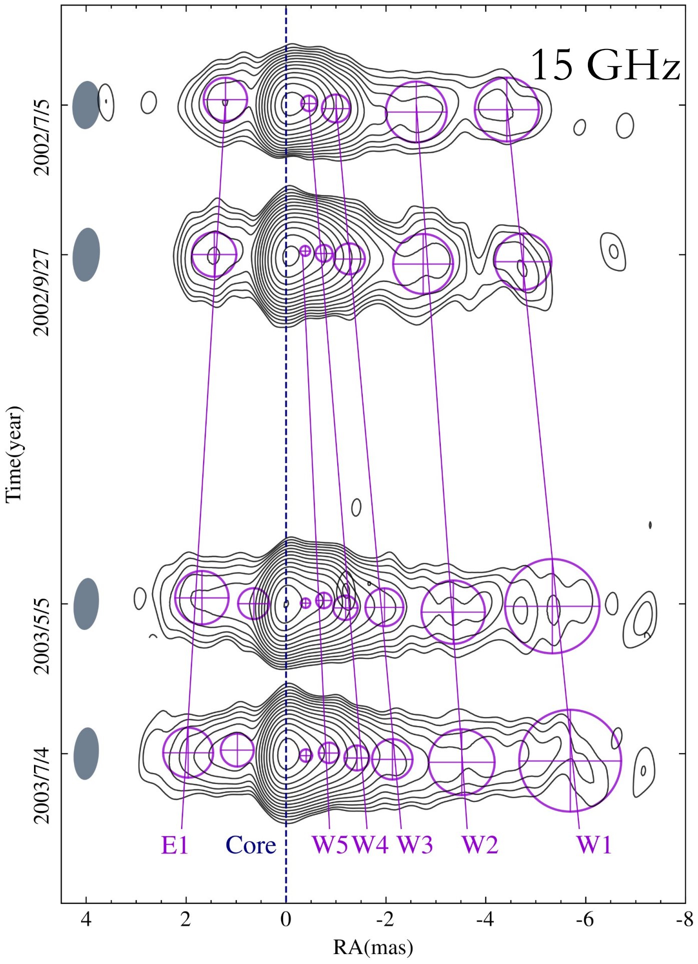

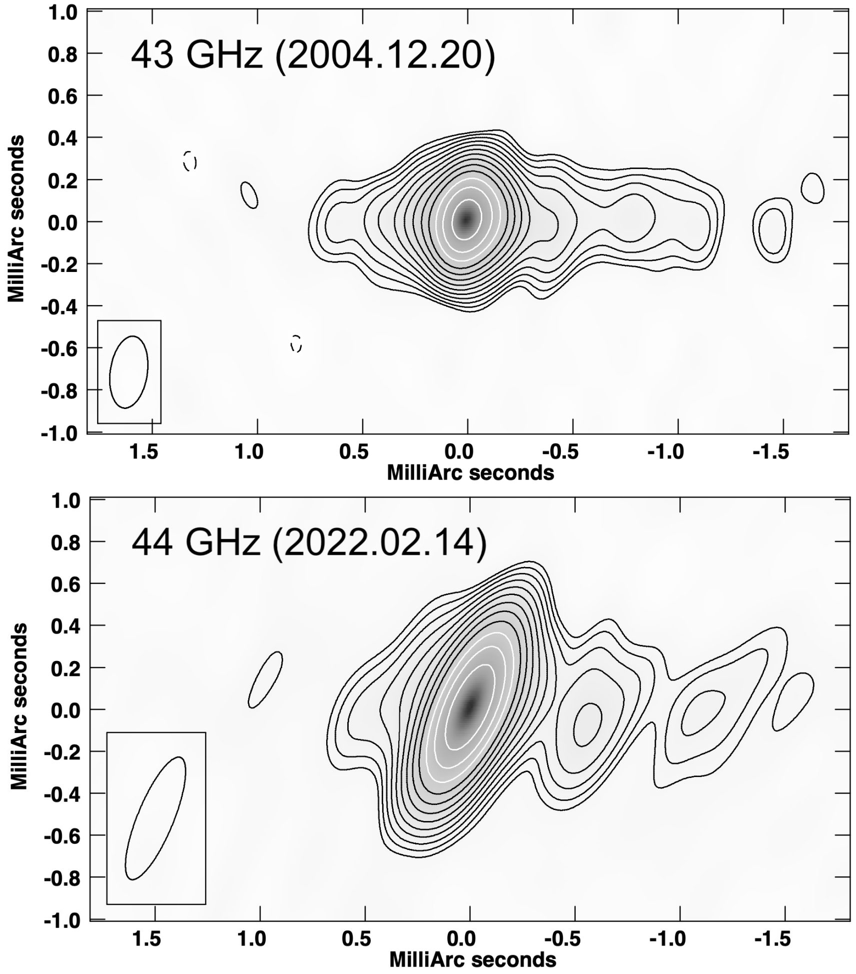

Yan et al. (2023)

SFPRed Image

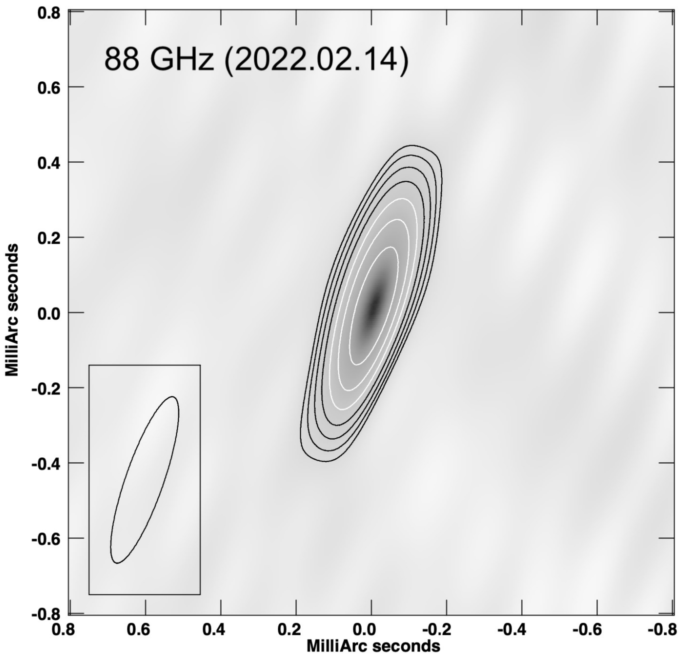

The first ever high-quality image at 88 GHz

- $d \approx 0.09$ mas $\approx 90R_s$
- $S \approx 60$ mJy
- $T_B \approx 1.3\times10^9$ K

2.3 Jet Viewing Angle

$$\beta_{\rm int} = \frac{\beta_{\rm app}}{\sin\theta + \beta_{\rm app}\cos\theta}$$

- θ: $54^\circ \lesssim \theta \lesssim 84^\circ$ $(71^\circ \pm 2^\circ)$

$$\beta_{\rm int} = \frac{1}{\cos\theta}\left(\frac{R^{1/(2-\alpha)} - 1}{R^{1/(2-\alpha)} + 1}\right),$$

- Piner et al. (2001) & Laing et al. (2014):

$$60^\circ \lesssim \theta \lesssim 76^\circ$$

- Weighted mean viewing angle: $68^\circ \pm 4^\circ$, based on the $71^\circ \pm 2^\circ$ and $63^\circ \pm 3^\circ$ (Piner et al. 2001)

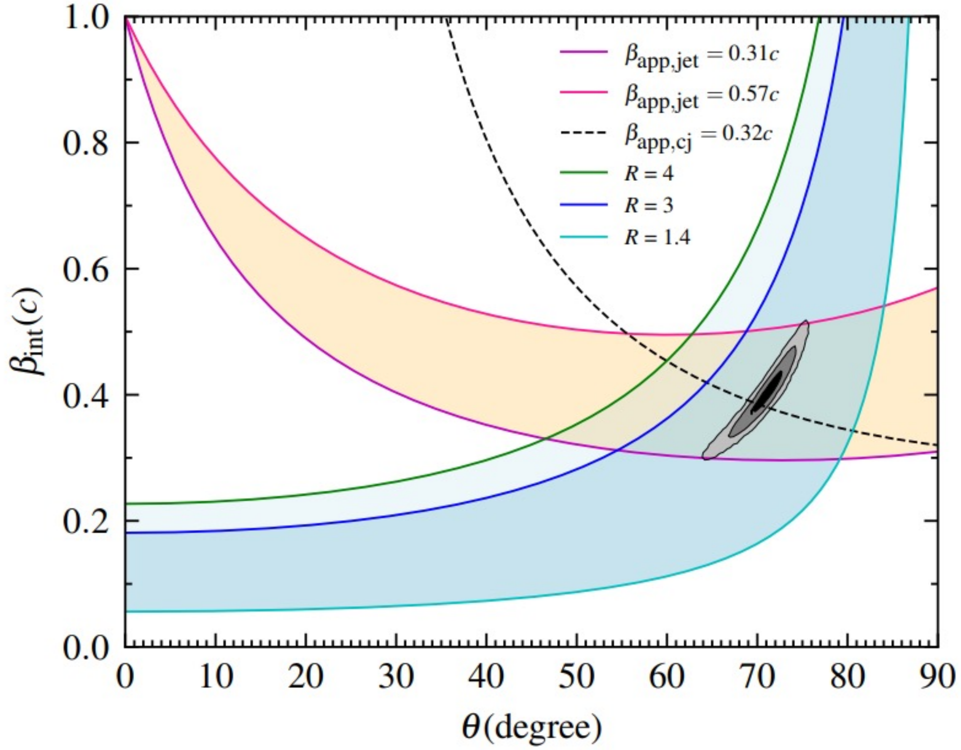

Yan et al. (2023, 2025)

2.4 Jet Collimation

- Parabolic shape: $W \propto r^{0.56\pm0.07}$
- $r_{\mathrm{break}} \ll r_{\mathrm{Bondi}}$, on subparsec scale of $\lesssim 1$ pc (≪ 100 pc)

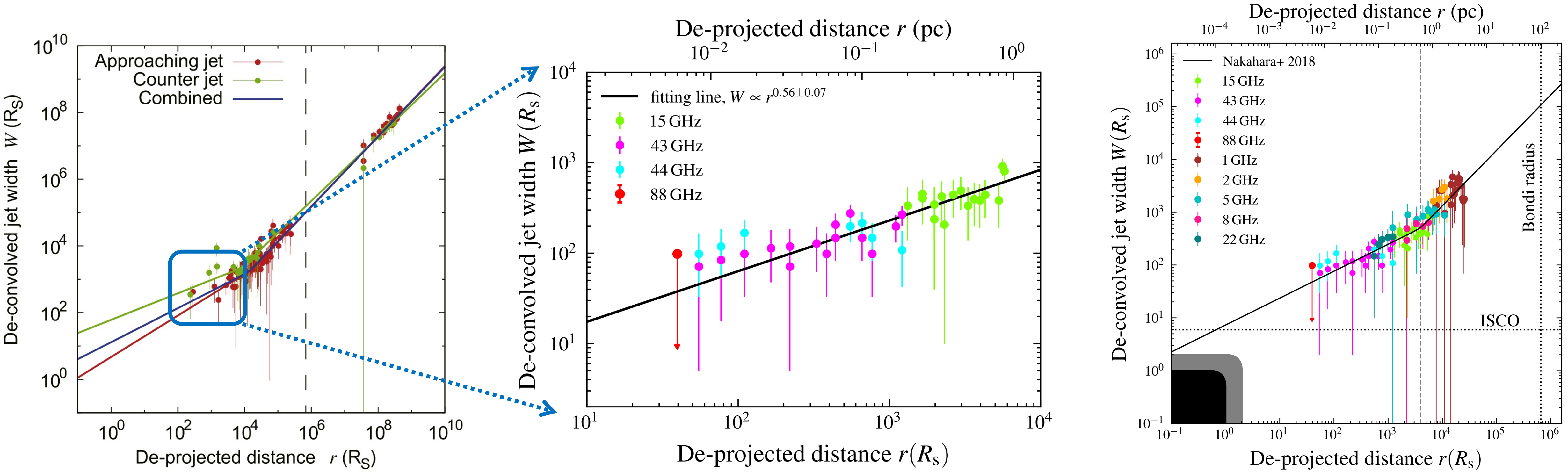

Nakahara et al. (2018)

Yan et al. (2023)

2.4 Jet Collimation

- To robustly determine the subparsec transition ($\lesssim$ 1 pc), we analyzed additional VLBA datasets and employed multiple methods:
  - Deconvolution (e.g., Asada & Nakamura 2012; Park et al. 2021, 2024)
  - Model fitting (e.g., Boccardi et al. 2021)
  - Using the multi-frequency core properties, i.e., core size and core shift (Hada et al. 2013)

Yan et al. (2025)

2.4 Jet Collimation

- The jet collimation is **indeed** already completed on the (sub)parsec scale of ~1pc
- The collimation profiles of the twin jets show a high degree of symmetry

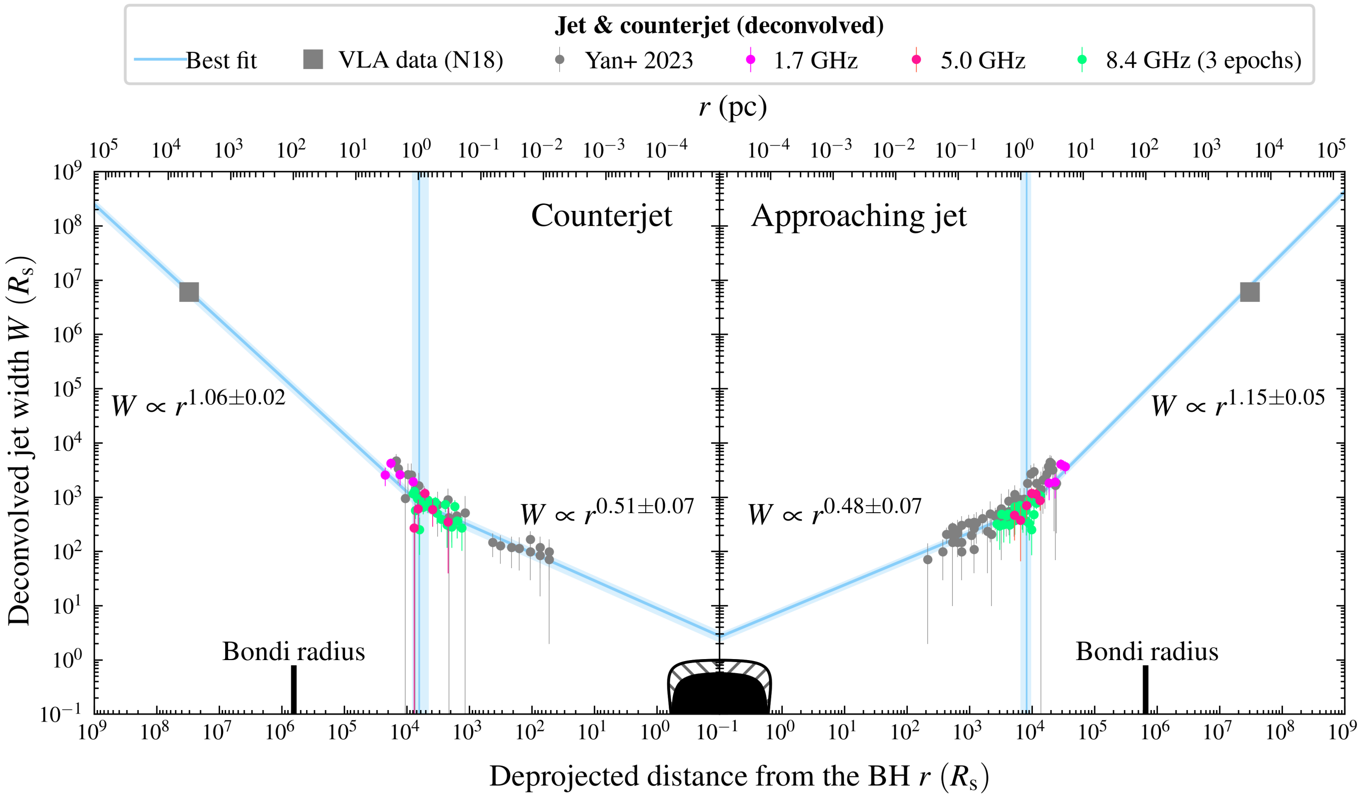

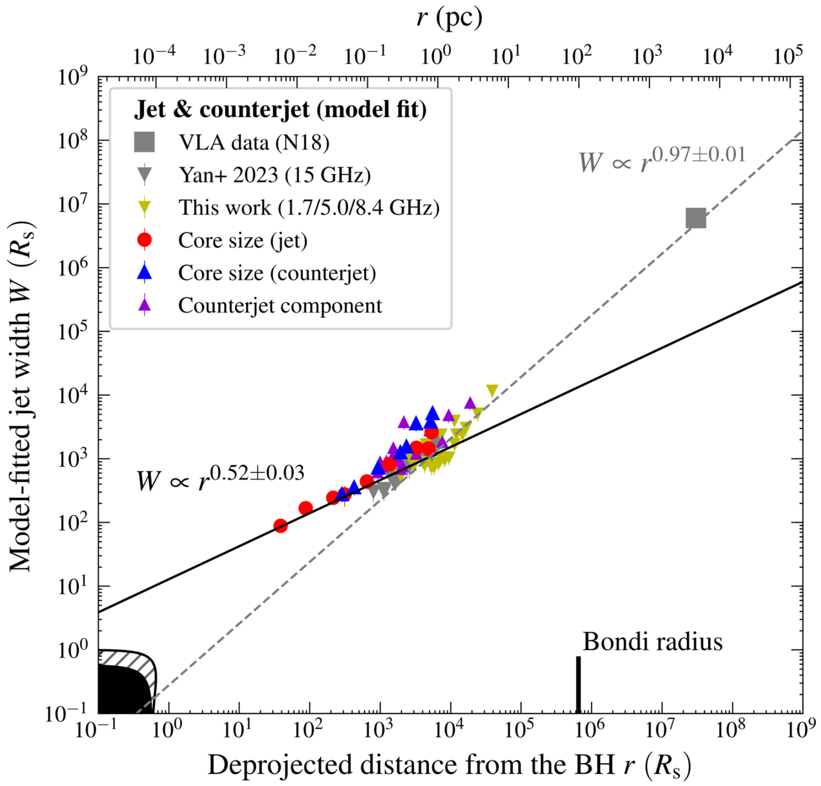

Yan et al. (2025)

2.5 Jet Acceleration

- Previous work (Piner et al. 2001):
  - The approaching jet: $0.52 \pm 0.07\ c$
- Yan et al. (2023):
  - Approaching: $0.31 \pm 0.14\ c \sim 0.59 \pm 0.40\ c$
  - Receding: $0.32 \pm 0.14\ c$

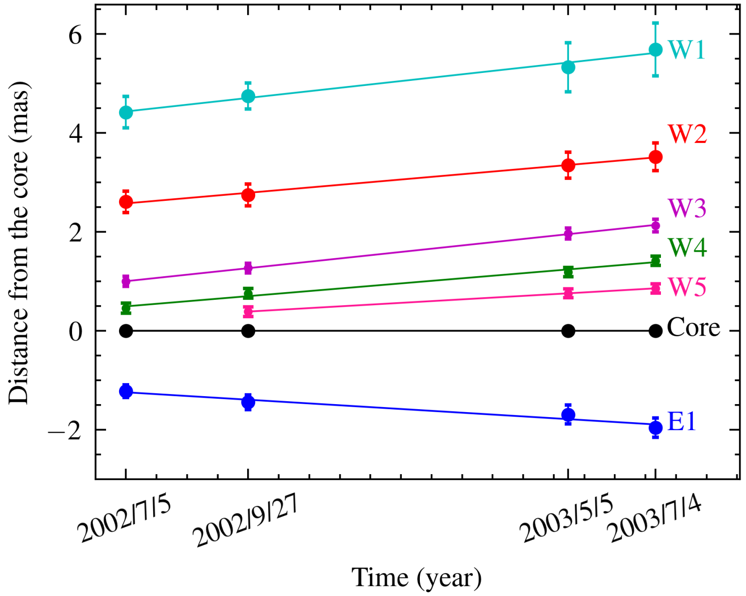

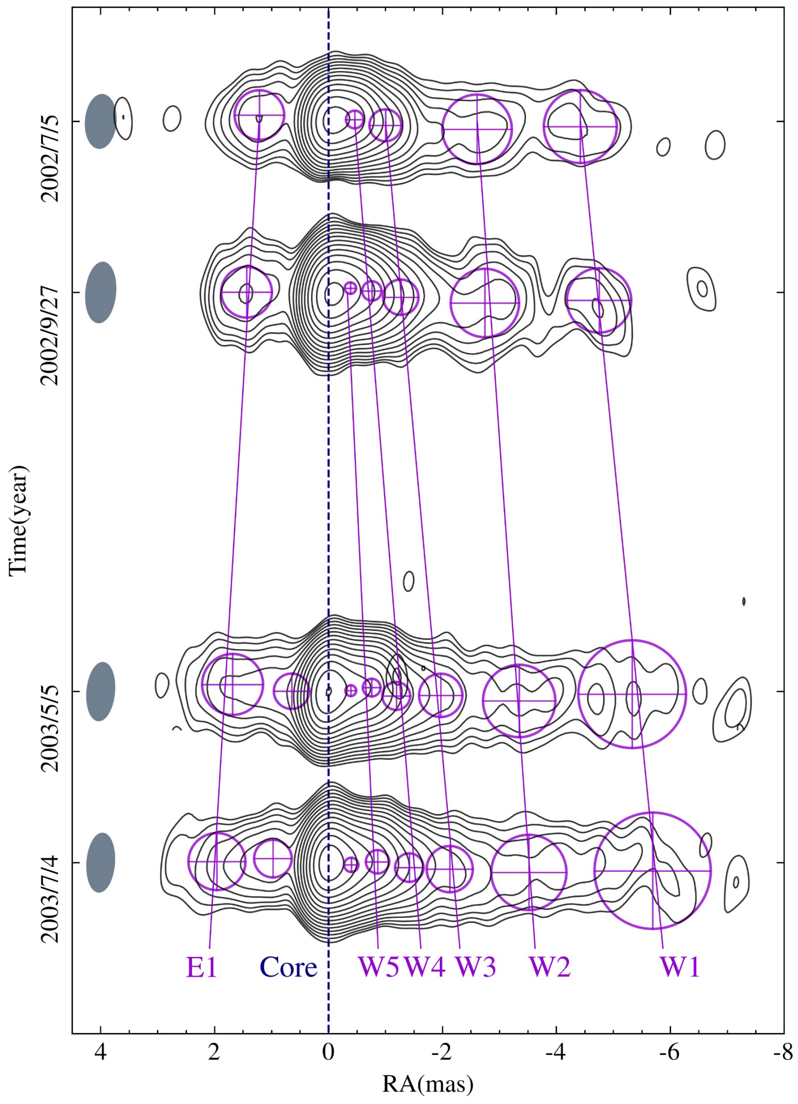

Yan et al. (2023)

2.5 Jet Acceleration

For a pair of intrinsically symmetric twin jets:

$$\beta_{\mathrm{int}} = \frac{1}{\cos\theta}\left(\frac{R_{\mathrm{B}}^{1/(2-\alpha)} - 1}{R_{\mathrm{B}}^{1/(2-\alpha)} + 1}\right)$$

Jet-to-counterjet brightness ratio

Spectral index

Jet viewing angle, ~68 deg

R_B

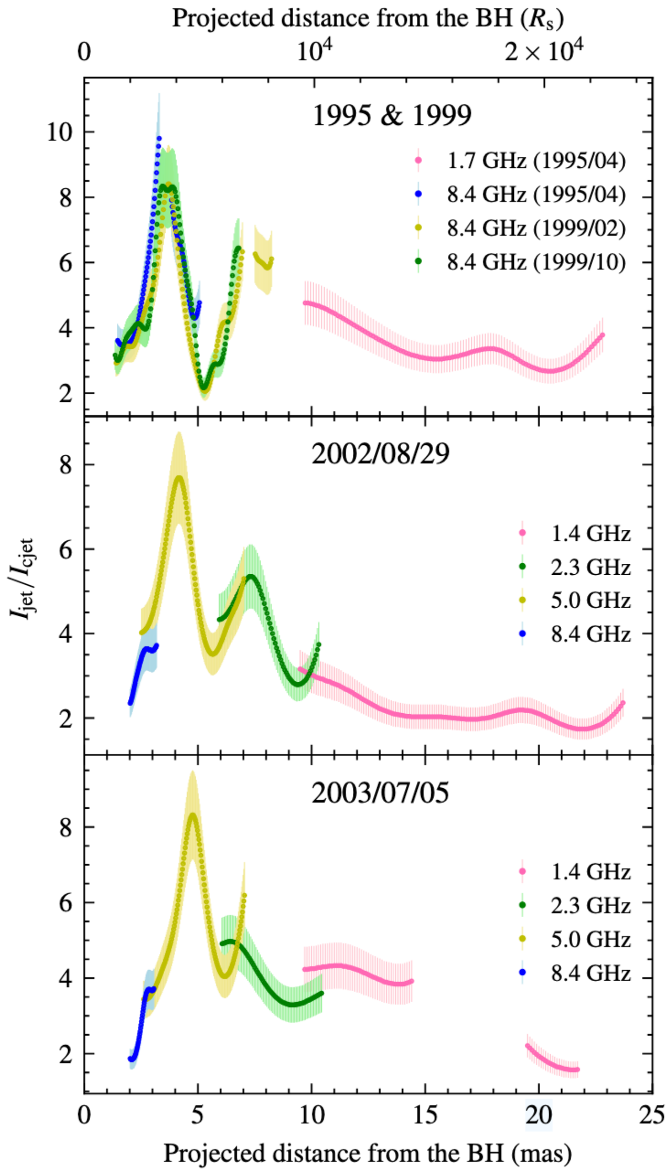
Projected distance from the BH (R_s)
0
10^4
2×10^4
1995 & 1999
1.7 GHz (1995/04)
8.4 GHz (1995/04)
8.4 GHz (1999/02)
8.4 GHz (1999/10)
2002/08/29
1.4 GHz
2.3 GHz
5.0 GHz
8.4 GHz
2003/07/05
1.4 GHz
2.3 GHz
5.0 GHz
8.4 GHz
I_{jet}/I_{cjet}
Projected distance from the BH (mas)

α

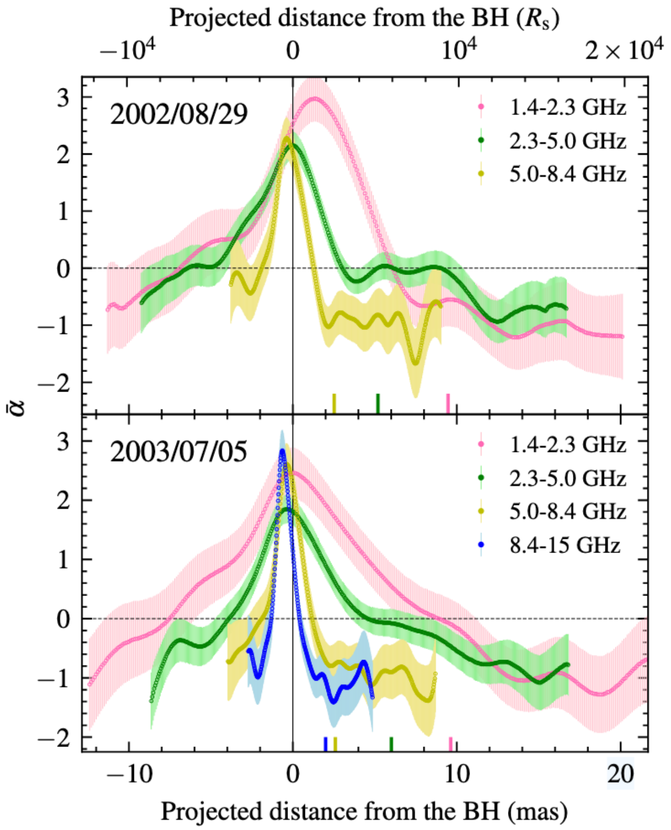
Projected distance from the BH (R_s)
-10^4
0
10^4
2×10^4
2002/08/29
1.4-2.3 GHz
2.3-5.0 GHz
5.0-8.4 GHz
2003/07/05
1.4-2.3 GHz
2.3-5.0 GHz
5.0-8.4 GHz
8.4-15 GHz
$\bar{\alpha}$
Projected distance from the BH (mas)

2.5 Jet Acceleration

$$\beta_{\mathrm{int}} = \frac{1}{\cos\theta}\left(\frac{R_{\mathrm{B}}^{1/(2-\alpha)}-1}{R_{\mathrm{B}}^{1/(2-\alpha)}+1}\right)$$

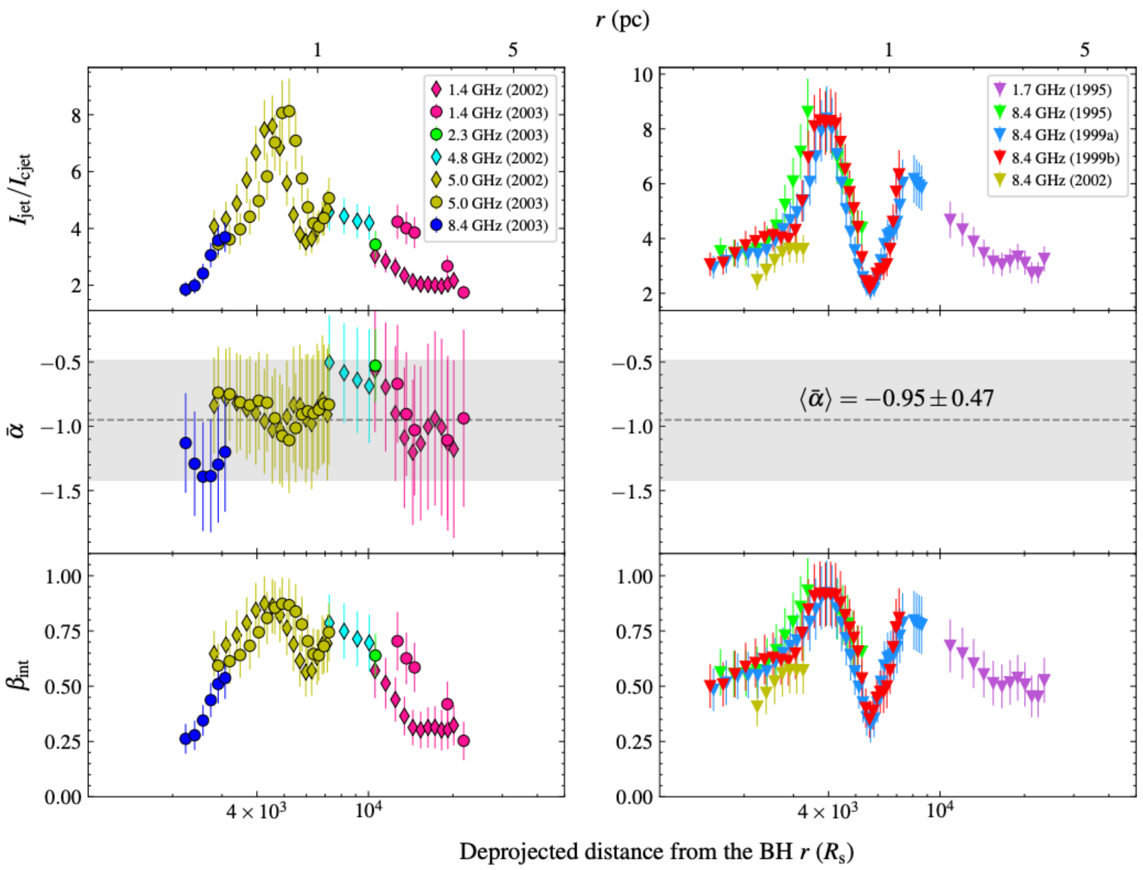

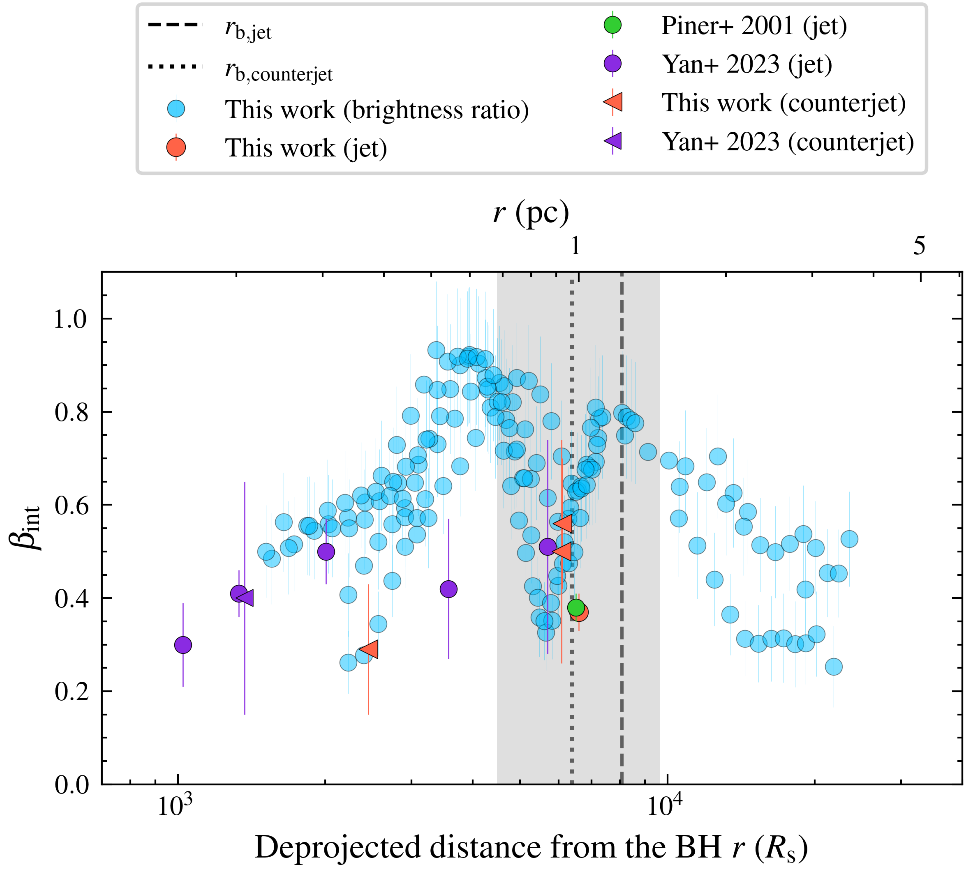

2.5 Jet Acceleration

- Jet reaches relativistic speeds at ~1 pc
- Coincide well with the jet collimation break location (~1 pc)
- Suggest a subparsec-scale co-spatial ACZ in NGC 4261

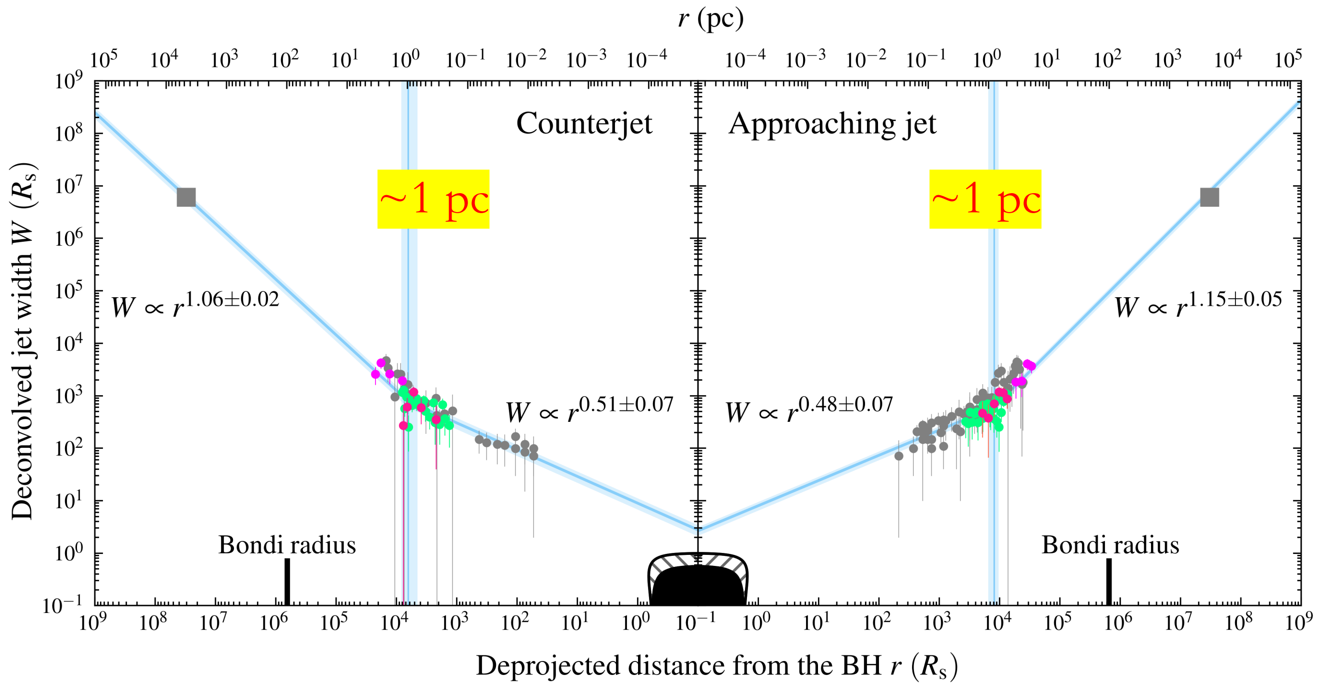

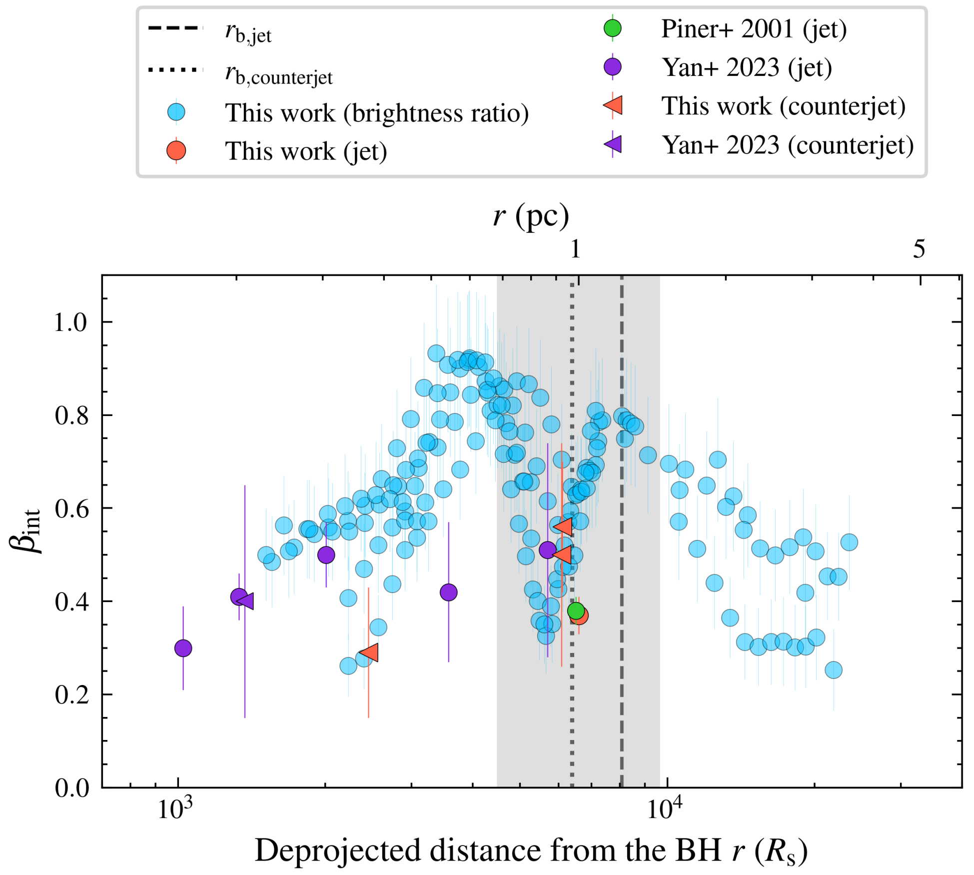

2.5 Jet Acceleration

➢ $\Gamma \propto r^{0.21\pm0.04}$ at distances of $(1-3)\times10^3 R_s$ vs. $\Gamma \propto r^{0.16\pm0.01}$ for M 87

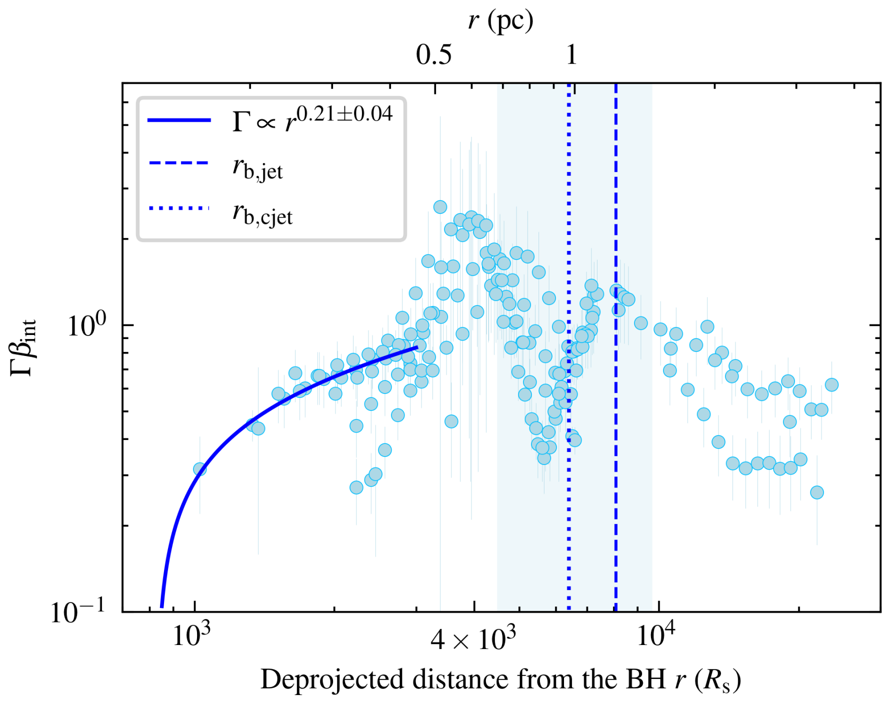

NGC 4261; Yan et al. (2025)

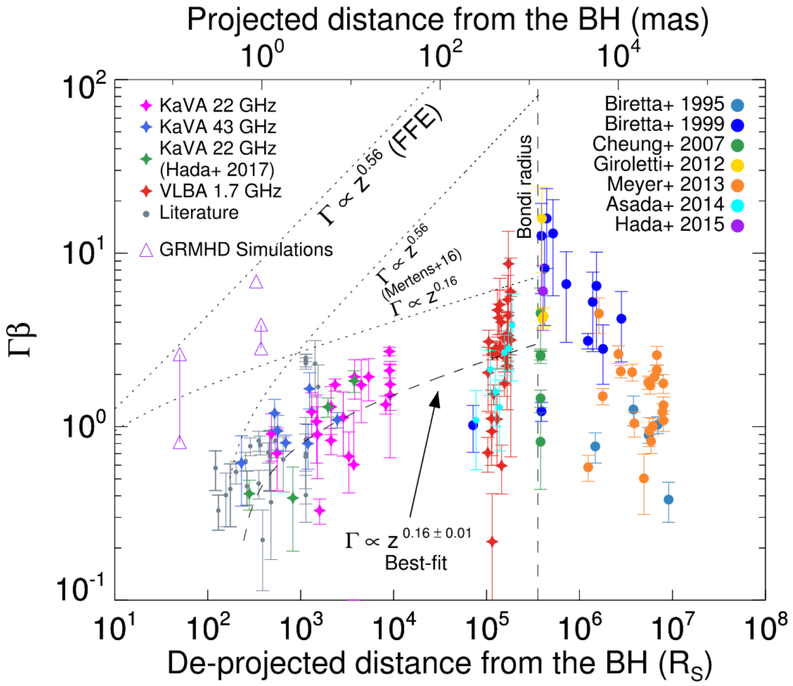

M 87; Park et al. (2019)

2.6 Recollimation Shock?

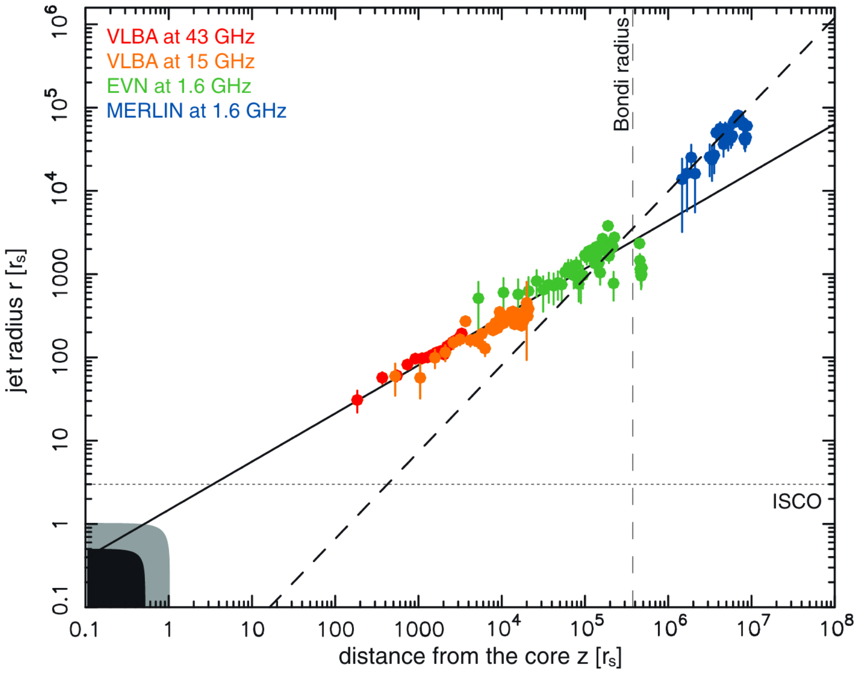

M87
(Asada et al. 2012)

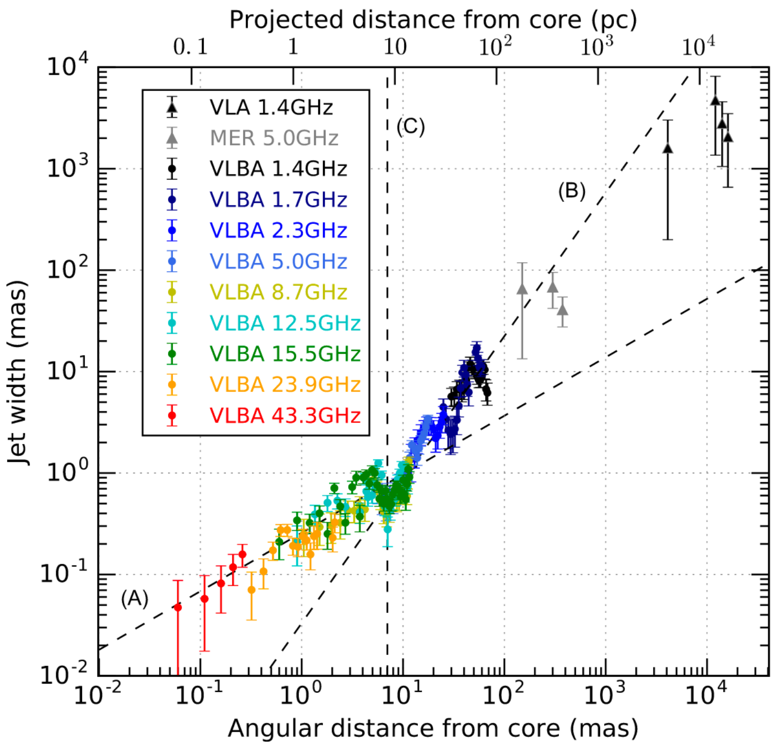

1H 0323+342
(Hada et al. 2018)

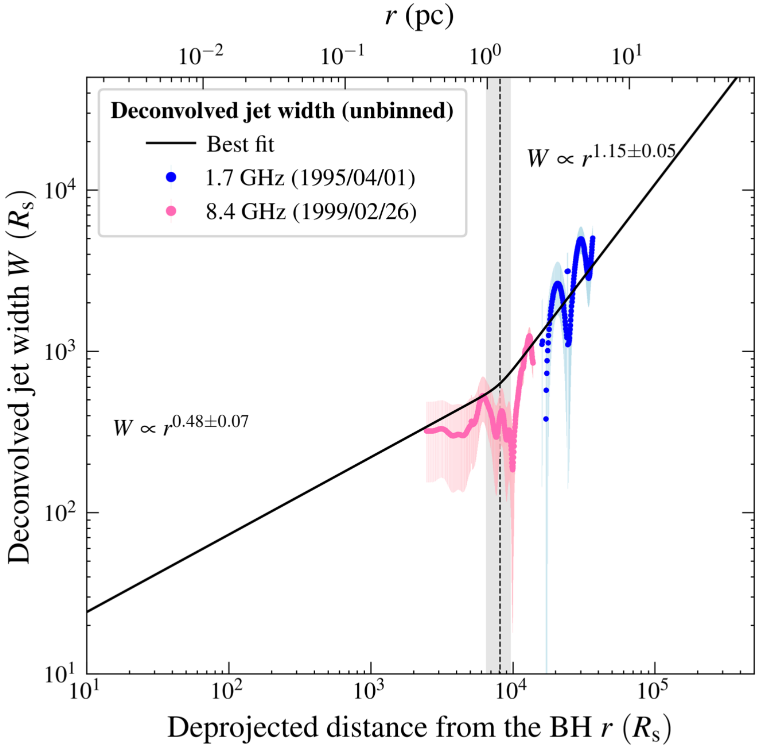

NGC 4261
Yan et al. (2025)

2.7 Discussion

- ➢ADAF
- ➢Wind → A (sub)parsec-scale ACZ
- ➢B field

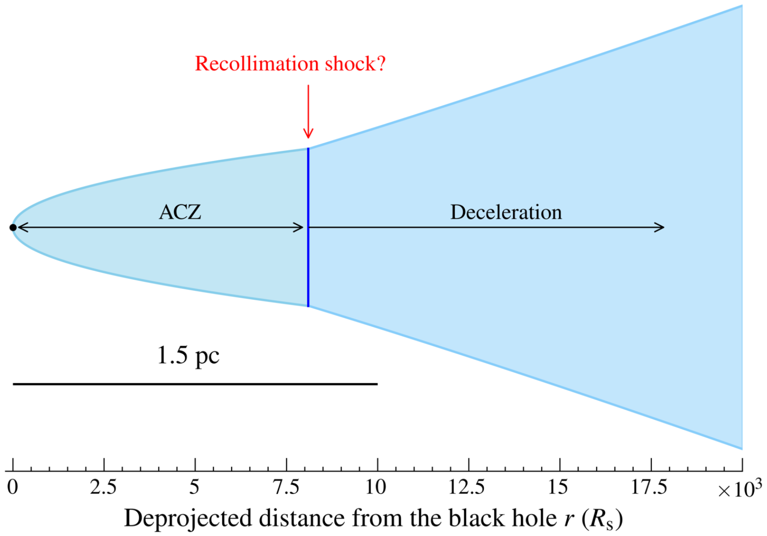

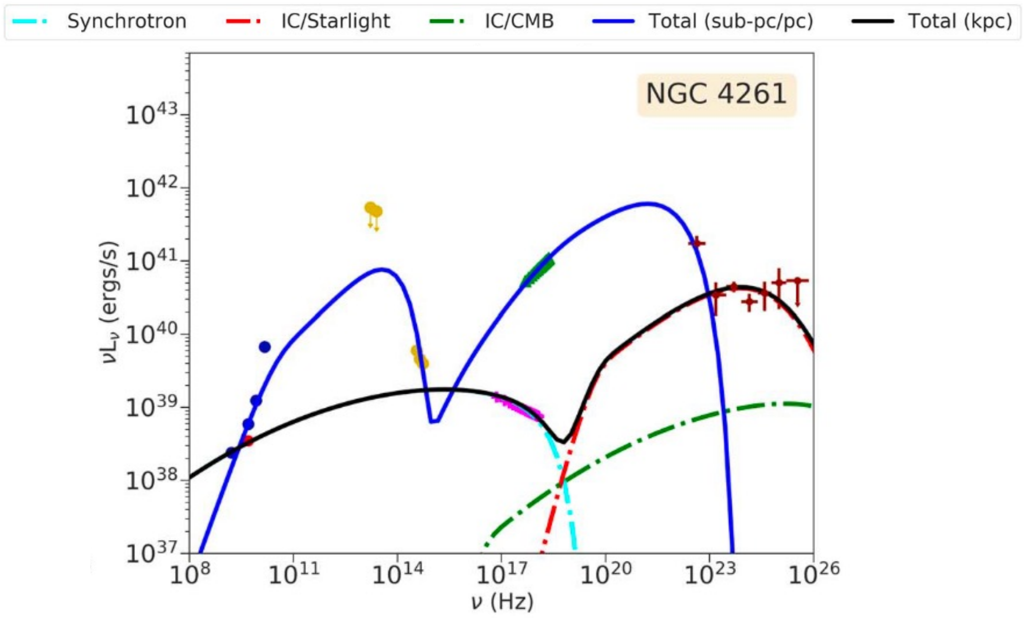

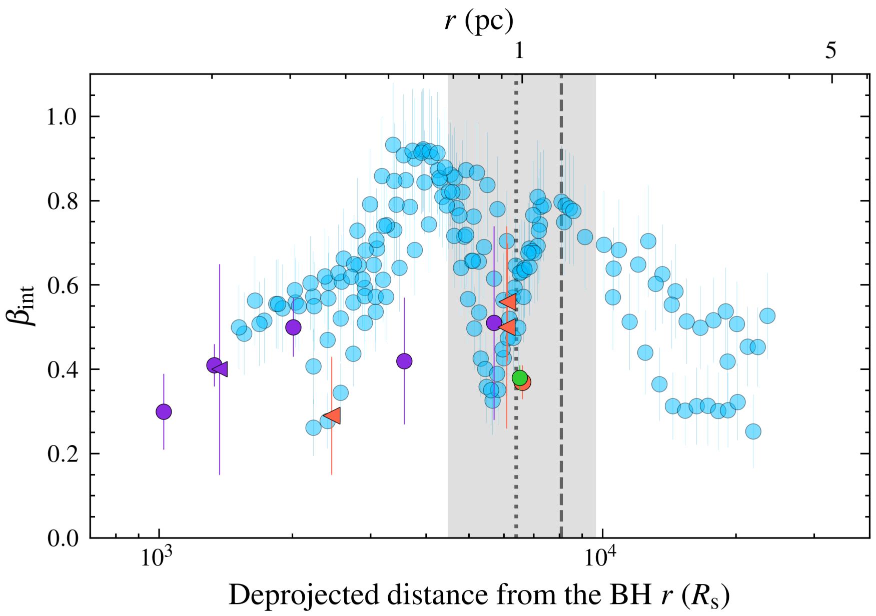

Menezes et al. (2020) ; Tomar et al. (2021)

A Brief Comparison with M 87

	M 87	NGC 4261
M_{BH} ($M_\odot$)	6.5×10^9	1.62×10^9
θ	$\sim18^\circ$	$\sim68^\circ$
Jet Collimation	Parabolic → Conical (~ 200 pc; ~ r_{Bondi})	Parabolic → Conical (~**1** pc; ≪ r_{Bondi}= 100 pc)
Jet Acceleration	Gradual acceleration ($\Gamma \propto r^{0.16\pm0.01}$; $\Gamma_{max} = 10$)	Gradual acceleration ($\Gamma \propto r^{0.21\pm0.04}$; $\Gamma_{max} = 2.6$)
Jet ACZ	~ 200 pc ~ r_{Bondi}	~1 pc ≪ r_{Bondi}
Recollimation Shock	Clearly observed at the end of the ACZ	A possible hint of the presence of recollimation shock at the end of ACZ
γ-ray Emission	High-energy γ-ray emission has been detected in these **two low-luminosity radio galaxies**	

Yan et al. (2025)

3. Summary and Outlook

- NGC 4261's ACZ may represent a scaled-down analogue of that in M 87

- NGC 4261 is the fifth radio-loud AGN showing compelling evidence of a co-spatial ACZ

- mm-VLBI observations with multi-band receivers + SFPR technique will play a key role in probing the innermost jet region of nearby LLAGNs

- Future works:
  - EAVN 6.7 GHz data (40 hours; observed)
  - HSA (VLBA+VLA27) 22/43 GHz data (8 hours; approved)

Thank you very much for your attention!

Sombrero Galaxy. Image Credit: NASA, ESA, CSA, STScI, Hubble Heritage Project (STScI, AURA)